



IJRASET

International Journal For Research in
Applied Science and Engineering Technology



INTERNATIONAL JOURNAL FOR RESEARCH

IN APPLIED SCIENCE & ENGINEERING TECHNOLOGY

Volume: 6 Issue: IV Month of publication: April 2018

DOI: <http://doi.org/10.22214/ijraset.2018.4688>

www.ijraset.com

Call:  08813907089

E-mail ID: ijraset@gmail.com

Liquid Phase Benzoylation of O-Xylene on Nano Mesoporous Lanthanum Aluminates

Marymol Moothedan¹, K. B. Sherly²

^{1,2} Regional Research Centre of M.G. University, Mar Athanasius College, Kothamangalam, Kerala, India, 686666

Abstract: Nano lanthanum aluminates synthesized by sol-gel method were used for the liquid phase benzoylation of o-xylene (o-Xyl) with benzyl chloride (BC) in a batch reactor at atmospheric pressure. Lanthanum aluminates were characterized in depth by Differential thermo gravimetric analysis (DTG), Differential scanning calorimetric analysis (DSC), X-ray diffraction (XRD), Fourier transform infrared spectroscopy (FTIR), N₂ sorption, transmission electron microscopy (TEM), temperature-programmed desorption using CO₂/NH₃ (CO₂-TPD/NH₃-TPD) and temperature-programmed reduction using H₂ (H₂-TPR) in order to relate its performances to the chemical and textural characteristics. Nano La₁₀Al₄O₂₁ was detected for lower aluminum precursor concentration and stable nano mesoporous LaAlO₃ becomes the major phase as the concentration increases. The band gap of LaAlO₃ and La₁₀Al₄O₂₁ was estimated from ultraviolet-visible (UV-Vis) spectrophotometry. Ac conductivity and dielectric measurement of lanthanum aluminates were also performed. The effect of catalyst concentration, reaction temperature, reaction time and o-Xyl/BC molar ratio on benzoylation of o-Xyl was studied over stable nano mesoporous LaAlO₃ and was extended to nano La₁₀Al₄O₂₁ at the optimized conditions. LaAlO₃ showed 92% and La₁₀Al₄O₂₁ showed 51% BC conversion at the following reaction conditions (catalyst to BC (w/w) = 0.1, o-Xyl/BC molar ratio =1:1, 433K, 2h, 1 atm). The acidity and mesoporous structure of LaAlO₃ appeared to be responsible for its good performance. Increase in catalyst concentration, reaction temperature and reaction time enhances the conversion of BC, whereas it decreases with the increase in o-Xyl/BC molar ratio. The Friedel-Crafts (FC) benzoylation reaction mechanism involves the formation of an electrophile (C₆H₅CH₂⁺) over an acidic lanthanum aluminate catalyst which attacks the O-Xyl ring resulting in the formation of 3,4 -dimethyl diphenyl methane.

Keywords: Benzoylation; Lanthanum aluminates; La₁₀Al₄O₂₁; Sol gel; Mesoporous;

I. INTRODUCTION

Rare earth aluminates have attracted keen interest over the years owing to their unique physical and chemical properties [1]. Among them lanthanum aluminates have attracted wide-spread attention in different frontier areas of research due to their outstanding potential in superconductors [2], radiation dosimetry [3], memory devices [4], semiconductor [5], thermal barrier coating [6] and heterogeneous catalysis [7].

In addition, when a mixed metal oxide attains mesoporosity with appreciable good surface area, it can play key role in many industrial applications [8]. Even though large varieties of mesoporous materials have been studied intensively, little attention have been paid to the synthesis of mesoporous mixed metal oxides and their application potentials. Lanthanum aluminate is generally synthesized via solid state reactions [9], co-precipitation [10] or polymer complexing plus combustion method [11]. But the environmentally benign citrate-sol gel method has been rarely employed.

The construction of C-C bond by FC benzoylation has revolutionized organic synthesis and chemical manufacturing [12]. The product, dimethyldiphenylmethanes (DMDPM) have many useful applications [13, 14]. To the best of our knowledge FC benzoylation by nano mesoporous lanthanum aluminates has not reported so far. FC benzoylation in the presence of homogeneous and heterogeneous catalysts, although giving better yields in industrial scale; these catalysts, however have several drawbacks such as toxicity, corrosiveness, less activity, moisture sensitivity etc [13, 15]. Thus we need a non-corrosive, non toxic, active heterogeneous solid catalyst, which can be synthesized in a convenient, cost-effective and environmentally friendly route. In this context, successful synthesis and utilization of mesoporous lanthanum aluminates is very much important.

II. EXPERIMENTAL

A. Catalyst preparation

All chemicals were analytical grade and were used without further purification. Lanthanum aluminates were synthesized by the modified citrate sol-gel method [16]. Citric acid was added to the premixed lanthanum and aluminum nitrate solution while stirring, such that molar ratio of acid/La+Al = 2. The solution was heated in a water bath until a viscous gel was obtained. The gel was dried at 110°C overnight to form a spongy material. The dried gel was calcined at 800°C for 6 hrs.

B. Catalyst Characterization

The thermal behavior of the dried gel was examined by DTG/DSC analysis using Perkin Elmer STA 6000 thermo gravimetric apparatus. The phases were identified by means of XRD with a RIGAKU D/MAX-C diffractometer using Cu K α radiation ($\lambda = 1.5405\text{\AA}$) at a scanning rate of 5° s^{-1} . Surface morphology was evaluated by TEM (HR-TEM-JEOL, JEM-2100). FT-IR studies were done in KBr medium using Thermo Nicolet Avatar 370 model FT-IR spectrophotometer. UV-Vis diffuse reflectance spectra were recorded over a wavelength range between 200 to 2000 nm using a Varian, Cary 5000 spectrometer. Surface properties were determined using Micromeritics Gemini VII surface area and porosity analyzer by N₂ adsorption at 77K, according to the standard Brunauer –Emmer-Teller (BET) method. The Lewis basicity and acidity were studied by CO₂-TPD, NH₃-TPD experiments using Micromeritics ChemiSorb 2750 pulse chemisorption apparatus. Reduction characteristics were analyzed by H₂-TPR analysis using the same Micromeritics chemisorption apparatus. Dielectric characterization was done by using Agilent 16451B Impedance analyzer in parallel mode at frequencies ranging from 40 Hz to 1 MHz.

C. Catalytic Activity

The catalytic activity of nano mesoporous lanthanum aluminates was tested for FC benzylation of o-Xyl with BC in solvent free liquid phase reaction. The benzylation was performed in liquid phase batch reactor consists of a round bottom flask with condenser, in a constant temperature oil bath with magnetic stirring. In typical run, appropriate amounts of o-Xyl and BC (1:1 and 5:1 molar ratio) was charged in the reactor along with 0.05 to 0.25 g catalyst. The reaction mixture was heated to 303 to 473 K under stirring for 30 to 190 min. Samples were withdrawn periodically and analyzed with a gas chromatograph (Perkin Elmer Clarus 650) fitted with a flame ionization detector and Elite 5 capillary column. Some selected runs were analyzed by GC-MS for product identification.

III. RESULTS AND DISCUSSION

A. Catalyst Characterization

1) *Thermal analysis:* Fig. 1 shows the results of thermal analysis of LaAlO₃ precursor prepared by citrate sol-gel method. The first weight loss of about 13%, at 100°C in the DTG curve is due to dehydration. The endothermic peak around 550°C in the DSC curve, accompanied by weight loss of about 16%, is due to the degradation of the residual citric acid and the elimination of residual CO₃²⁻ and NO₃⁻ ions [17]. The weight loss of about 5% at 780°C is associated with further oxidation of the sample.

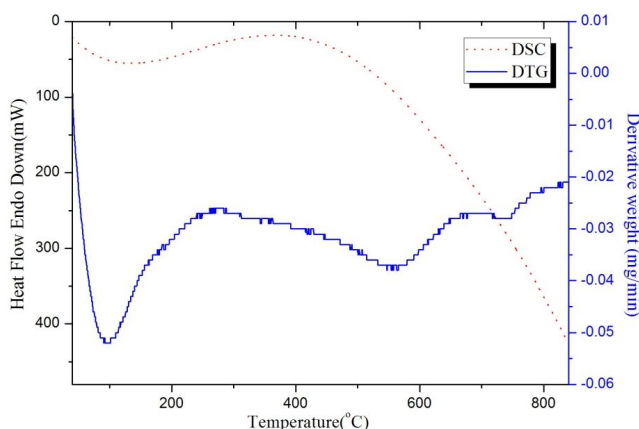


Fig. 1 Differential thermo gravimetric analysis and differential scanning calorimetric analysis of LaAlO₃ precursor

2) *Formation of LaAlO₃:* Fig. 2 shows XRD patterns of samples prepared by citrate sol gel method and calcined at 800°C for 6 hrs. Secondary phase of orthorhombic La₁₀Al₄O₂₁ were detected (JCPDS 39-0009) for the sample prepared by using 0.030M Al(NO₃)₃. LaAlO₃ phase with rhombohedral structure (JCPDS 31-0022) begins to appear as the concentration of Al(NO₃)₃ increases and becomes the major phase as the concentration reaches to 0.05M. Formation of La₂CO₃ and La(OH)₃ were also identified at lower Al(NO₃)₃ concentrations (0.005M-0.020M).

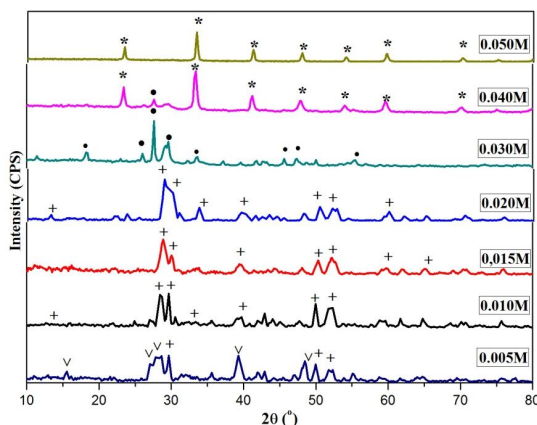


Fig. 2 XRD patterns of samples prepared by citrate sol-gel method using varying concentration of $\text{Al}(\text{NO}_3)_3$ calcined at 800°C for 6 hrs (* - LaAlO_3 , •- $\text{La}_{10}\text{Al}_4\text{O}_{21}$, +- La_2CO_3 , v- $\text{La}(\text{OH})_3$)

3) *FT-IR spectroscopy*: Fig. 3 shows the FT-IR spectra of LaAlO_3 and $\text{La}_{10}\text{Al}_4\text{O}_{21}$. The broad absorption band at 3430 cm^{-1} is associated with the O-H stretching vibrations and the bands at $1200\text{--}1000\text{ cm}^{-1}$ were assigned to O-H bending vibrations of molecular water [18]. The bands around $880\text{--}440\text{ cm}^{-1}$ in the spectra were assigned to Al-O vibrational modes [19]. The peaks around 2349 cm^{-1} and $1617\text{--}1493\text{ cm}^{-1}$ can be assigned to angular vibration modes and stretching modes of carbonate groups [20]. The results indicate the presence of immense amount of adsorbed water and CO_2 on $\text{La}_{10}\text{Al}_4\text{O}_{21}$ compared to LaAlO_3 .

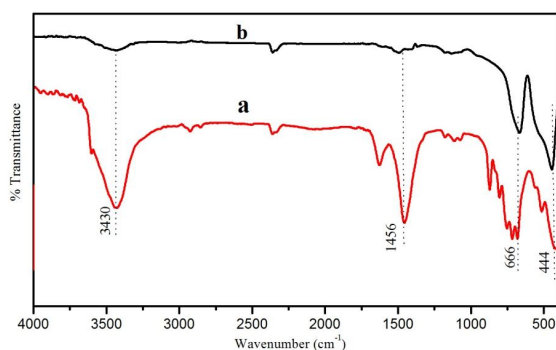


Fig. 3 FT-IR spectra of nano (a) $\text{La}_{10}\text{Al}_4\text{O}_{21}$ (b) LaAlO_3

4) *Optical absorbance*: UV-Vis absorption study was carried out in order to determine the band gap of nano lanthanum aluminates. The optical band gap was estimated by plotting $(\alpha h\nu)^2$ versus photon energy ($h\nu$), based on the relation $\alpha h\nu = A (h\nu - E_g)^{1/2}$, where α is the absorption coefficient, A is a constant, E_g is the band gap [21], Fig. 4. The higher optical band gap of orthorhombic $\text{La}_{10}\text{Al}_4\text{O}_{21}$ (5.2 eV) compared to rhombohedral LaAlO_3 (4.6 eV) may be due to difference in their lattice constants [22].

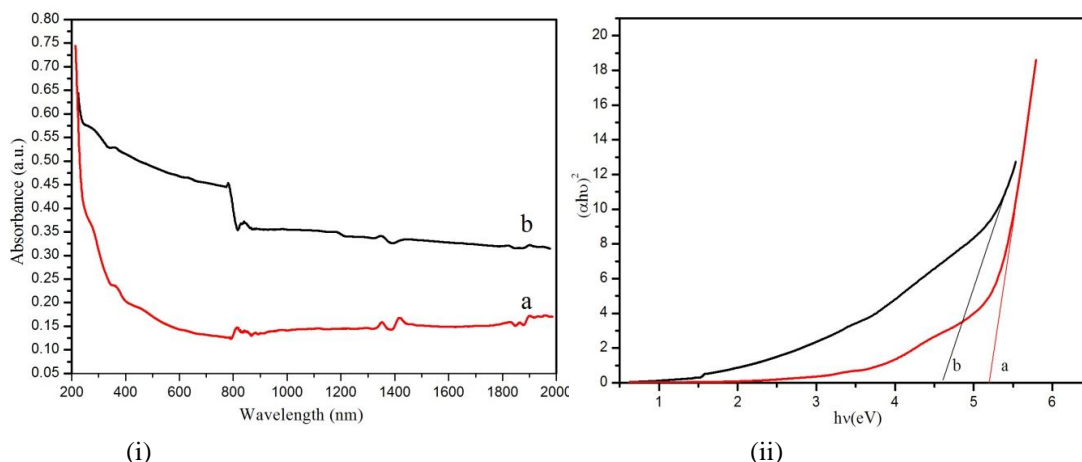


Fig. 4 (i) UV-Vis absorption spectra and (ii) Tauc plot of nano (a) $\text{La}_{10}\text{Al}_4\text{O}_{21}$ (b) LaAlO_3

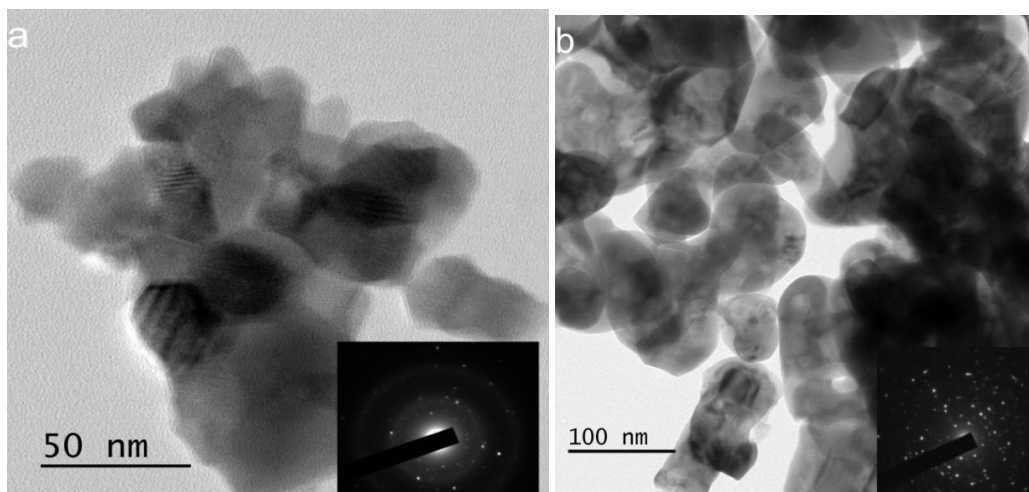


Fig. 5 TEM morphology of nano (a) $\text{La}_{10}\text{Al}_4\text{O}_{21}$ (b) LaAlO_3

5) *Particle size and Morphology*: The size and morphology of $\text{La}_{10}\text{Al}_4\text{O}_{21}$ and LaAlO_3 nano particles were shown in the Fig. 5 (a) & b. In contrast to $\text{La}_{10}\text{Al}_4\text{O}_{21}$ powder, LaAlO_3 powder has a rather regular shape and is weakly agglomerated. However, $\text{La}_{10}\text{Al}_4\text{O}_{21}$ has less particle size (35-40 nm) compared to LaAlO_3 (65-70 nm).

6) *Surface area* : The total surface area of lanthanum aluminate nanoparticles were obtained by Brunauer–Emmett–Teller (BET) method using N_2 adsorption-desorption isotherm data. All experimental parameters of BET surface area analysis were summarized in Table I. Nano $\text{La}_{10}\text{Al}_4\text{O}_{21}$ has large surface area with large pore diameter compared to nano LaAlO_3 . Fig. 6 shows the BJH plots for N_2 adsorption-desorption isotherm and pore size distribution of lanthanum aluminate nano particles. Typical type V isotherm with H_3 type hysteresis loops at high P/P_0 value is observed for nano LaAlO_3 , characteristics of large mesopores [23]. Hysteresis loop in nano $\text{La}_{10}\text{Al}_4\text{O}_{21}$ may due to tensile strength effect [24].

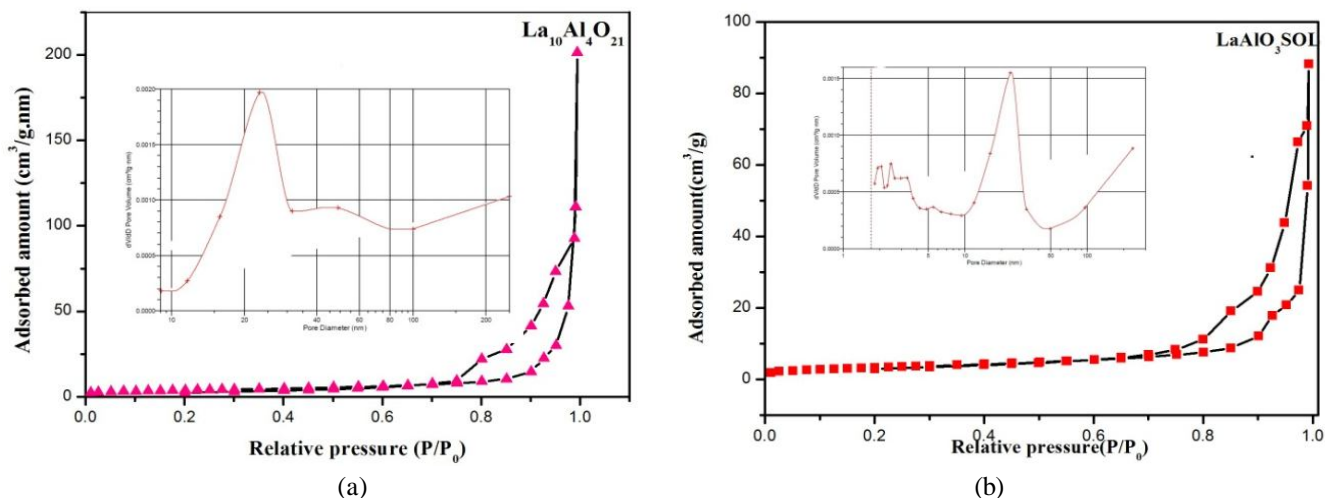


Fig. 6 N_2 adsorption-desorption isotherm and pore size distribution of nano (a) $\text{La}_{10}\text{Al}_4\text{O}_{21}$ (b) LaAlO_3

Table I Experimental Parameters Of Bet Surface Area Analysis Of Nano Lanthanum Aluminates

Sample	BET Surface area (m^2/g)	BJH pore volume (cm^3/g)	BJH adsorption average pore diameter (nm)	BJH desorption average pore diameter (nm)
$\text{La}_{10}\text{Al}_4\text{O}_{21}$	13.4	0.31	82.2	100.8
LaAlO_3	12.4	0.31	48.7	28.2

Table II Lewis Sites Distribution In Nano Lanthanum Aluminate Evaluated On The Basis Of CO₂-Tpd/ NH₃-Tpd

Sample	Basic sites (μmolg ⁻¹)				Acid sites (μmolg ⁻¹)			
	Weak	Strong	Very strong	Total	Weak	Strong	Very strong	Total
La ₁₀ Al ₄ O ₂₁	13.9	61.4	120.9	196.2	41.7	600.08	290.11	931.9
LaAlO ₃	58.3	-	-	58.3	57.8	83.3	900.2	1041.3

7) *Surface acidity and basicity* : For metal oxides, the metal ions are Lewis acid sites whereas the surface lattice oxygen are Lewis basic sites. CO₂-TPD, NH₃-TPD profiles of lanthanum aluminates is shown in the Fig. 7. From the figure it is clear that LaAlO₃ surface has higher no of Lewis acidic sites and less no of Lewis basic sites compared to La₁₀Al₄O₂₁. According to desorption temperature Lewis sites in lanthanum aluminates are categorized into weak (<200°C), strong (200-600°C) and very strong sites (>600°C) [25], Table. II. Lewis basic sites with weak strength mostly corresponds to OH⁻ groups on the catalyst surface, while those with strong and very strong strength are related to the oxygen of Mⁿ⁺O²⁻ ion pair and isolated O²⁻ anions [26]. Lewis acidity depends on the existence of exposed metal cations at the surface [27].

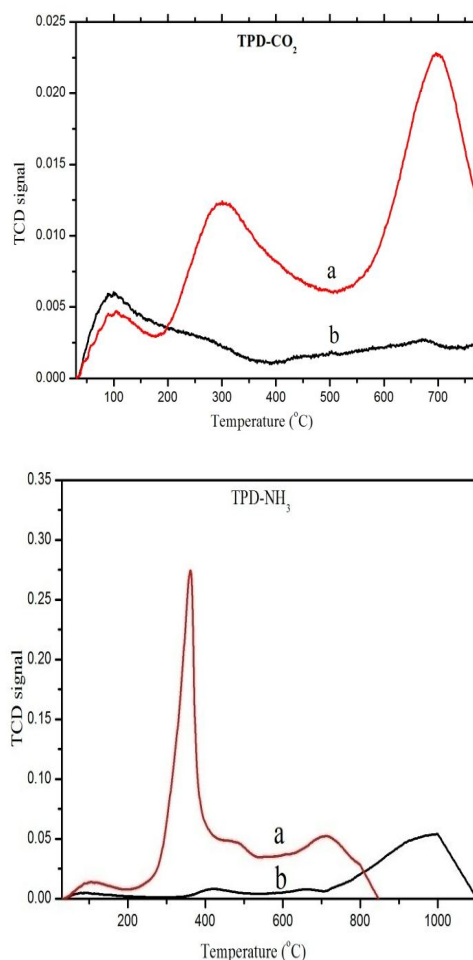


Fig. 7 CO₂-TPD, NH₃-TPD profile of nano (a) La₁₀Al₄O₂₁ (b) LaAlO₃

8) *Reducibility*: The H₂-TPR profiles of lanthanum aluminates are shown in the Fig. 8. In this figure H₂ consumption equates to oxidation of H₂ molecules by lanthanum aluminates. Thus we found that La₁₀Al₄O₂₁ has less reducing ability compared to LaAlO₃. The values of H₂ consumption at different peak temperatures are listed in Table III. The higher amount of H₂ consumption shows the higher amount of reactive oxygen in LaAlO₃ [28].

Table iii Quantitative H₂-Tpr Analysis Of Nano Lanthanum Aluminate

Sample	Peak temperature(°C)	H ₂ consumption (μmolg ⁻¹)
La ₁₀ Al ₄ O ₂₁	662.5	180.51
	678.9	136.9
LaAlO ₃	691.8	297.8
	732.2	135.9

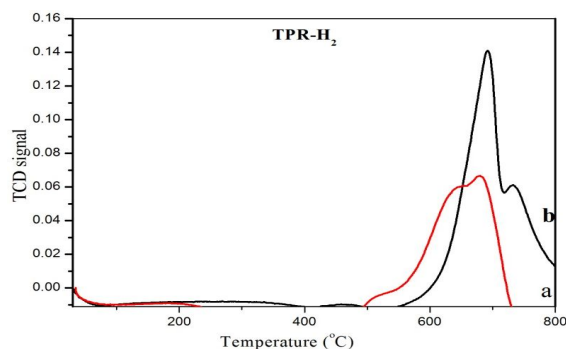


Fig. 8 H₂-TPR profile of nano mesoporous (a) La₁₀Al₄O₂₁ (b) LaAlO₃

9) *Dielectric Properties and ac Conductivity Measurement:* The effect of ac frequency on capacitance, loss tangent and dielectric constant at room temperature for lanthanum aluminates are shown in Fig. 9. Dielectric relaxation observed in lanthanum aluminates may be due to the fact that the species contributing to the polarizability are lagging behind the applied field at higher frequency [29]. Higher capacitance and dielectric constant of LaAlO₃ may be due to its mesoporous nature and higher interface, orientation, ionic and electronic polarizations compared to La₁₀Al₄O₂₁.

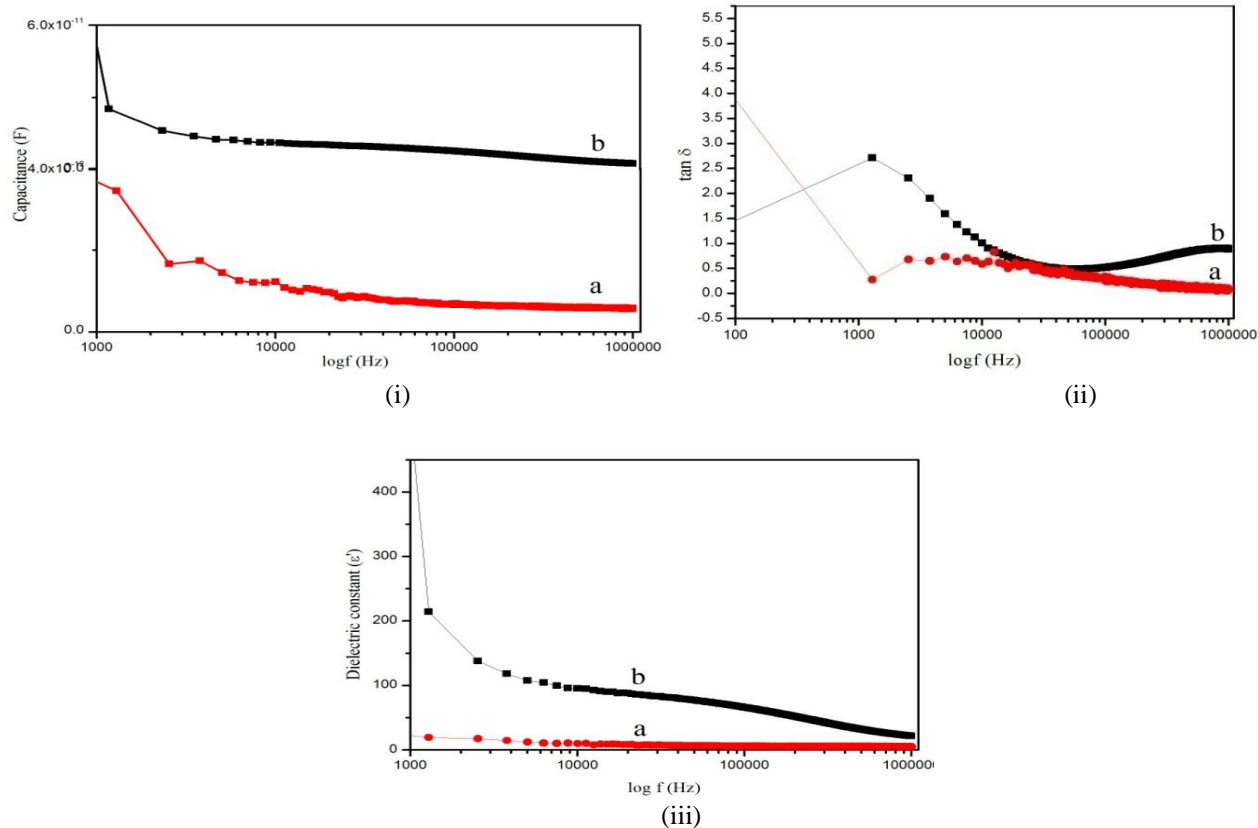


Fig. 9 Frequency dependent variation of (i) capacitance, (ii) loss tangent and (iii) dielectric constant of nano (a) La₁₀Al₄O₂₁ (b) LaAlO₃

To understand the conduction mechanism, the variation of ac conductivity as a function of frequency is measured, Fig. 10. As depicted in the Fig.10, ac conductivity increases with increasing frequency. Low percolation probability and low moisture content of nano mesoporous LaAlO₃ may be the reason for its very high ac conductivity compared to nano La₁₀Al₄O₂₁[30].

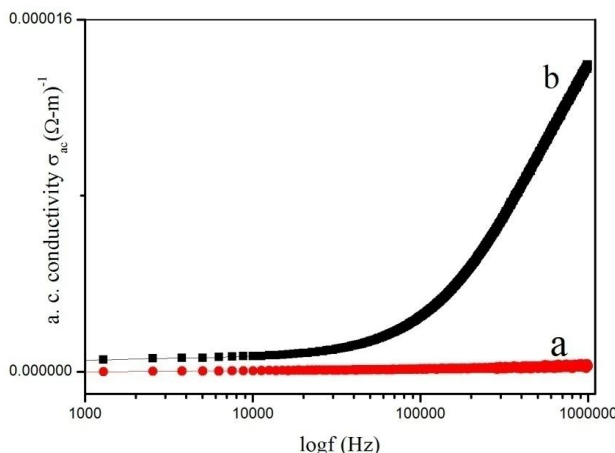


Fig. 10 Frequency dependent variation of ac conductivity in nano (a) La₁₀Al₄O₂₁ (b) LaAlO₃

B. Catalytic Reactions

The FC benzylation of o-Xyl with BC was carried out using stable nano mesoporous LaAlO₃ at different reaction temperature, catalyst weight and reaction time for 1:1 and 5:1 molar ratio of o-Xyl/BC and extended to La₁₀Al₄O₂₁ at the optimized conditions. Benzylation of o-Xyl was also carried out in the absence of catalyst and no obvious BC conversion was detected

1) *Thermal Analysis:* The effect of catalyst concentration in the range of 0.05-0.25 g mol⁻¹ of BC on the conversion of BC is studied at 433 K for 2 h of reaction for different molar ratios of o-Xyl/BC over nano mesoporous LaAlO₃ as catalyst. The catalysts to BC ratios are changed by keeping the constant concentration of BC in the reaction mixture. When the catalyst to BC ratio is increased from 0.05 to 0.25, the conversion of BC is also found to increase from 14 to 100 % for 1:1 o-Xyl/BC molar ratio and 40 to 100% for 5:1 o-Xyl/BC molar ratio. A reaction rate plateau appears when the catalyst weight exceeds 0.2 g mol⁻¹ of BC for 1:1 o-Xyl/BC molar ratio and 0.25 g mol⁻¹ of BC for 1:5 o-Xyl/BC molar ratios. These results confirm that with an increase in catalyst loading the conversion of BC increases because of the increase in the total number of acidic sites available for the reaction [15]. 3,4-Dimethyl Diphenylmethane (3, 4-DMDPM) was detected as the major product.

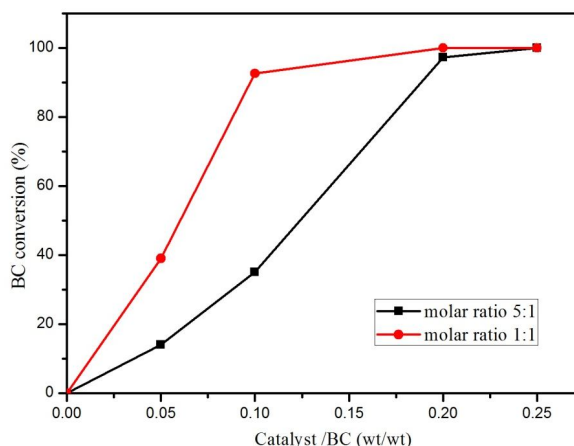


Fig. 11 Effect of catalyst/BC molar ratio on the conversion of BC for different molar ratios of o-Xyl/BC

2) *Effect of Reaction Temperature:* The temperature dependency of this reaction at the following reaction conditions (catalyst to BC (w/w) = 0.1, 2h, 1 atm) for different molar ratios of o-Xyl/BC is shown in Fig. 12. BC conversion over LaAlO₃ as catalyst increases steadily from 20 to 100% for 1:1 o-Xyl/BC molar ratio and 1 to 54% for 5:1 o-Xyl/BC molar ratio as the temperature is raised from 302 to 473 K.

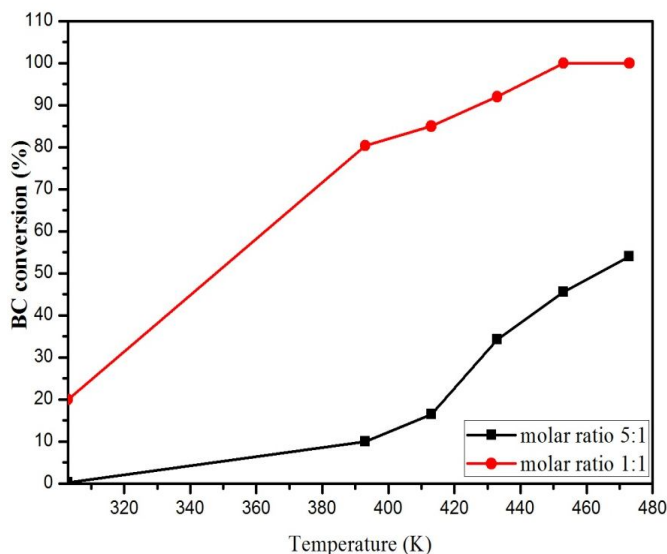


Fig. 12 Effect of reaction temperature on the conversion of BC for different molar ratios of o-Xyl/BC

3) *Effect of reaction Time:* The relationship between conversion of BC and reaction time for benzylation of o-Xyl over LaAlO_3 and $\text{La}_{10}\text{Al}_4\text{O}_{21}$ catalysts is illustrated in Fig. 13 at the following reaction conditions (catalyst to BC (w/w) = 0.1, o-Xyl/BC molar ratio = 1:1, 433K, 1 atm). LaAlO_3 gave higher conversion compared to $\text{La}_{10}\text{Al}_4\text{O}_{21}$. The conversion of BC over LaAlO_3 is found to be increased with the increase in the reaction time and reaches a maximum (92%) in 2 h of the run. $\text{La}_{10}\text{Al}_4\text{O}_{21}$ exhibit comparatively lower activity (51%) in this reaction. Large no of acidic sites and mesoporous structure of LaAlO_3 may be responsible for higher catalytic activity. The catalytic activity correlated well with their reducing ability, since the variation in the activities seems to follow the change in the reducing ability. This redox property was expected to play an important role for initiating benzyl carbocation ($\text{C}_6\text{H}_5\text{CH}_2^+$) for the reaction [13].

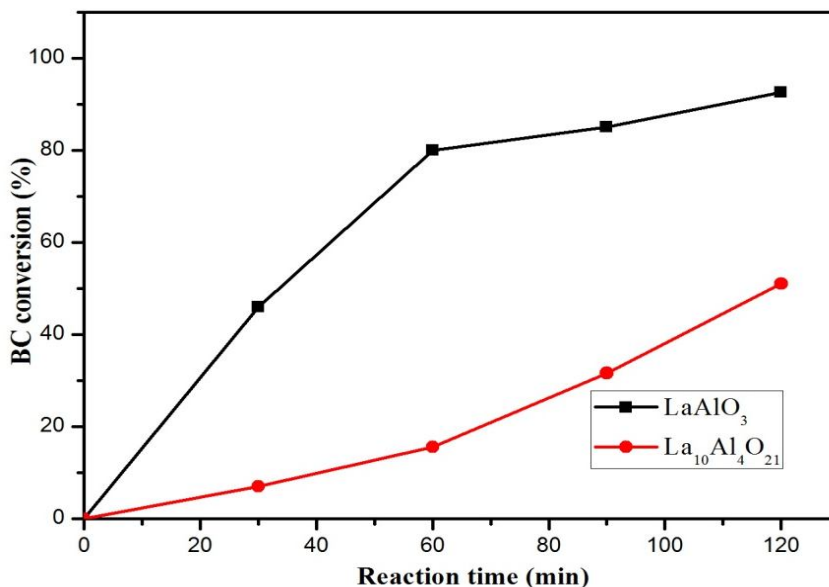


Fig. 13 Reaction time versus BC conversion over lanthanum aluminates

4) *Effect of o-Xyl/BC molar ratio:* Fig.14 shows the effect of varying the o-Xyl/BC molar ratio in the reaction mixture on the activity of nano mesoporous LaAlO_3 at a fixed BC concentration at the following reaction conditions (catalyst to BC (w/w) = 0.1, 433K, 1 atm). An increase in the BC conversion is observed with the decrease in o-Xyl/BC molar ratio. The study indicates that using excess o-Xyl results into fast deactivation of active sites, which may be attributed to passivation of active sites by strong adsorption of excessive o-Xyl molecule.

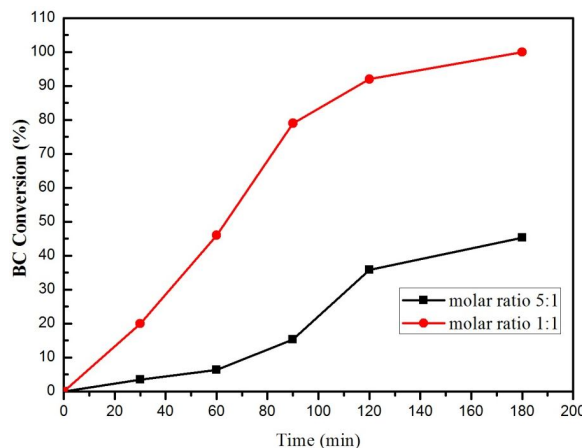


Fig. 14 Effect of o-Xyl/BC molar ratio on the conversion of BC

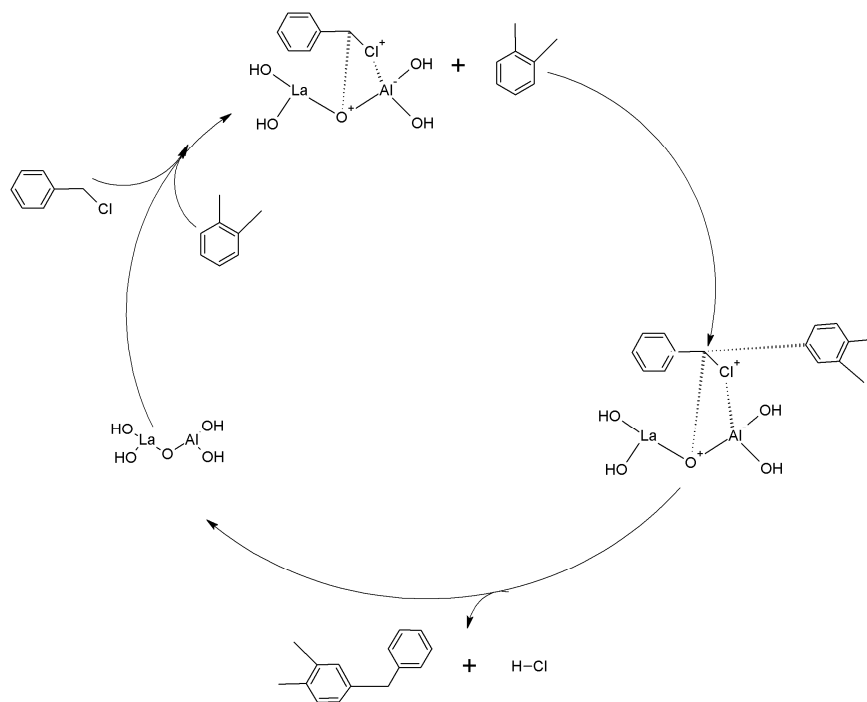


Fig. 15 Proposed reaction mechanism for the benzylation of o-Xyl using lanthanum aluminate catalyst

- 5) *Proposed Reaction Mechanism:* Generally benzylation of aromatics takes place by electrophilic aromatic substitution. A schematic diagram of the catalytic cycle for the benzylation of o-Xyl using lanthanum aluminate catalyst is represented in Fig. 15. The figure suggests that acidic LaAlO_3 polarizes the BC molecule into an electrophile ($\text{C}_6\text{H}_5\text{CH}_2^+$) which then attacks the o-Xyl ring resulting in the formation of 3, 4-DMDPM.

IV. CONCLUSIONS

Sol-gel method is used to prepare nano crystalline lanthanum aluminate powders. $\text{La}_{10}\text{Al}_4\text{O}_{21}$ developed at lower aluminum precursor concentration changes to stable LaAlO_3 as concentration increases. XRD and FTIR analysis confirmed the formation of LaAlO_3 and $\text{La}_{10}\text{Al}_4\text{O}_{21}$. $\text{La}_{10}\text{Al}_4\text{O}_{21}$ found to have lower particle size and higher surface area compared to LaAlO_3 . Mesoporous structure of LaAlO_3 and macroporous structure of $\text{La}_{10}\text{Al}_4\text{O}_{21}$ was revealed from BJH isotherm. UV-Vis absorption spectrometric data revealed large band gap of $\text{La}_{10}\text{Al}_4\text{O}_{21}$ (5.2 eV) in comparison with LaAlO_3 (4.6 eV). CO_2 -TPD, NH_3 -TPD and H_2 -TPR analysis results indicate small basicity, high acidity and high reduction potential of LaAlO_3 related to $\text{La}_{10}\text{Al}_4\text{O}_{21}$. LaAlO_3 found to have high ac conductivity and large dielectric constant compared to $\text{La}_{10}\text{Al}_4\text{O}_{21}$. Nano mesoporous LaAlO_3 was found to be an efficient catalyst

compared to nano $\text{La}_{10}\text{Al}_4\text{O}_{21}$ in the benzylation of o-Xyl. LaAlO_3 showed 92% BC conversion where as nano $\text{La}_{10}\text{Al}_4\text{O}_{21}$ exhibits 51% BC conversion at the same experimental conditions. The higher activity of LaAlO_3 may be attributed to its stronger acidic sites and mesoporous structure. The higher yield of product can be achieved by increasing reaction parameters such as; reaction temperature, catalyst concentration and reaction time, while the conversion is found to decrease with increase in molar ratio of o-Xyl/BC. The formation of 3, 4-DMDPM is explained by an electrophilic attack of the benzyl cation ($\text{C}_6\text{H}_5\text{CH}_2^+$) on the o-Xyl ring whose formation is facilitated by the stronger acid sites of catalyst.

V. ACKNOWLEDGMENT

The authors gratefully acknowledge UGC, New Delhi for pro-viding FIP to one of the authors Marymol Moothedan and also acknowledge the support of the Principal, Mar Athanasius College, Kothamangalam for providing infrastructure facilities. The technical assistance from SAIF, CUSAT were also acknowledged.

REFERENCES

- [1] L. Vasylechko, A. Senyshyn, and U. Bismayer, Perovskite-Type Aluminates and Gallates, Handbook on the Physics and Chemistry of Rare Earths, Vol. 39, Netherlands: North-Holland, 2009.
- [2] Bin Liu, Feng Yuan, Xiao Hu, "Impurity induced resonance states at the superconducting interface $\text{LaAlO}_3/\text{SrTiO}_3$ ", Journal of Physics and Chemistry of Solids, vol. 72, pp.380–383,2011.
- [3] V.H. Oliveira, N.M. Khaidukov, E.C. Silva, L.O. Faria, "Study of TL properties of $\text{LaAlO}_3:\text{Ce},\text{Dy}$ crystals for UV dosimetry", Radiation Measurements, vol.46, pp.1173–1175, 2011.
- [4] X.B. Lu, P.F. Lee, J.Y. Dai, "Effects of forming gas annealing on the memory characteristics of Ge nanocrystals embedded in LaAlO_3 high-k dielectrics for flash memory device application", Thin Solid Films, vol.513, pp.182–186, 2006.
- [5] X.B. Lu, H.B. Lu, J.Y. Dai, Z.H. Chen, M. He, G.Z. Yang, H.L.W. Chan, C.L. Choy, "Oxygen pressure dependence of physical and electrical properties of LaAlO_3 gate dielectric", Microelectronic Engineering, vol.77, pp. 399–404,2005.
- [6] Zahra Negahdari, Monika Willert-Porada, Florian Scherm, "Thermal properties of homogenous lanthanum hexaaluminate/alumina composite ceramics", Journal of the European Ceramic Society, vol. 30, pp. 3103–3109, 2010.
- [7] Xiaoguang Ren, Jiandong Zheng, Yongji Song, Ping Liu, "Catalytic properties of Fe and Mn modified lanthanum hexaaluminates for catalytic combustion of methane", Catalysis Communications, vol. 9, pp. 07–810, 2008.
- [8] Nabanita Pal, Manidipa Paul, Asim Bhaumik, "New mesoporous perovskite ZnTiO_3 and its excellent catalytic activity in liquid phase organic transformations", Applied Catalysis A: General, vol. 393, pp. 153–160, 2011.
- [9] N. Alves, W.B. Ferraz, L.O. Faria, "Synthesis and investigation of the luminescent properties of carbon doped lanthanum aluminate (LaAlO_3) for application in radiation dosimetry", Radiation Measurements, vol. 71, pp. 90–94, 2014.
- [10] Tomasz Brylewski, Mirosław M. Bućko, "Low-temperature synthesis of lanthanum monoaluminate powders using the co-precipitation–calcination technique", Ceramics International, vol. 39, pp. 5667–5674, 2013.
- [11] Shuai Li, Bill Bergman, Zhe Zhao, "Synthesis and characterization of lanthanum aluminate powders via a polymer complexing plus combustion route", Materials Chemistry and Physics, vol.132, pp. 309–315, 2012.
- [12] Magnus Rueping, Boris J. Nachtsheim, "A review of new developments in the Friedel–Crafts alkylation – From green chemistry to asymmetric catalysis", Beilstein J. Org. Chem., vol. 6, pp. 1-24, 2010.
- [13] Farook Adam, Adil Elhag Ahmed, "The benzylation of xylenes using heterogeneous catalysts from rice husk ash silica modified with gallium, indium and iron," Chemical Engineering Journal, vol. 145, pp. 328–334, 2008.
- [14] Chitralakha Khatri, Manish K. Mishra, Ashu Rani, "Synthesis and characterization of fly ash supported sulfated zirconia catalyst for benzylation reactions", Fuel Processing Technology, vol. 91, pp. 288–1295, 2010.
- [15] Ganapati D. Yadav, Shashikant B. Kamble, "Friedel–Crafts green alkylation of xylenes with tert-butanol over mesoporous superacid UDCaT-5", Chemical Engineering Research and Design, vol. 90, pp. 1322–1334, 2012.
- [16] X.-S. Liu, Jiqing Lu, L.-Y. Jin, M.-F. Luo, "High surface area $\text{Ce}_0.9\text{Cu}_{0.1}\text{O}_{2-5}$ and $\text{Ce}_0.9\text{Mn}_{0.1}\text{O}_{2.5}$ solid solutions for CO and HCHO oxidation", Indian J. Chemistry, vol. 48, pp. 1352-1357, 2009.
- [17] Y. B. R. D. Rajesh, R. S. Dubey, "Sol-Gel Synthesis and Characterization of Nanocrystalline Spinel LiMn_2O_4 For Battery Applications", Nanoscience and Nanoengineering, vol. 1, pp. 139-141, 2013.
- [18] Shantanu K. Behera, Prashant K. Sahu, Swadesh K. Pratihar, Santanu Bhattacharyya, "Phase evolution in gel-precipitated LaAlO_3 ceramics", Journal of Physics and Chemistry of Solids, vol. 69, pp. 2041-2046, 2008.
- [19] Yebin Xu, Guohua Huang, Hua Long, "Synthesis of lanthanum aluminate via the ethylenediaminetetraacetic acid gel route", Ceramics international, vol. 29, pp. 837-840, 2003.
- [20] G.C.C. Costa, R. Muccillo, "Synthesis of lanthanum beta-alumina powders by the polymeric precursor technique", Ceramics International, vol. 34, pp. 1703–1707, 2008.
- [21] Chen B, Yu J, Liang X., "LaAlO3 hollow spheres: synthesis and luminescence properties", Langmuir, vol. 27, pp. 11654-9, 2011.
- [22] M. A. Humayun, M. A. Rashid, F. A. Malek, A. N. Hussain, "Effect of lattice constant on band-gap energy and optimization and stabilization of high-temperature $\text{In}_x\text{Ga}_{1-x}\text{N}$ quantum-dot lasers", Journal of Russian Laser Research, vol. 33, pp. 387-394, 2012.
- [23] Weilun Wang, Peng Liu, Ming Zhang, Jiashan Hu, Feng Xing, "The Pore Structure of Phosphoaluminate Cement", Open Journal of Composite Materials, vol. 2, pp. 104-112, 2012.
- [24] Ali Sdiri, Teruo Higashi, Samir Bouaziz, Mourad Benzina, "Synthesis and characterization of silica gel from siliceous sands of southern Tunisia", Arabian Journal of Chemistry, vol. 7, pp. 486–493, 2014.



- [25] Yan, J., Yu, D., Sun, P., Huang, H., “Alkaline earth metal modified NaY for lactic acid dehydration to acrylic acid: Effect of basic sites on the catalytic performance original research article”, *Chin. J. Catal.*, vol. 32, pp. 405-411, 2011.
- [26] Ligu Wang, Yubo Ma, Ying Wang, et al., “Efficient synthesis of glycerol carbonate from glycerol and urea with lanthanum oxide as a solid base catalyst”, *Catalysis Communications.*, vol. 12, pp. 1458-1462, 2011.
- [27] Johannes A. Lercher, Christian Grundling, Gabriele Eder-Mirth, “Infrared Studies of the surface acidity of oxides and zeolites using adsorbed probe molecules”, *Catalysis today*, vol. 27, pp. 353-376, 1996.
- [28] María Haidy Castaño, Rafael Molina and Sonia Moreno, “Oxygen Storage Capacity and Oxygen Mobility of Co-Mn-Mg-Al Mixed Oxides and Their Relation in the VOC Oxidation Reaction”, *Catalysts*, vol. 5, pp. 905-925, 2015.
- [29] Abdul Samee Fawzi, A.D. Sheikh, V.L. Mathe, “Structural, dielectric properties and AC conductivity of $Ni_{(1-x)}Zn_xFe_2O_4$ spinel ferrites”, *Journal of Alloys and Compounds*, vol. 502, pp. 231–237, 2010.
- [30] E. Rodríguez-Castellón J. Jiménez-Jiménez, A. Jiménez-Lopez, P. Maireles-Torres, J.R. Ramos-Barrado, D.J. Jones, J. Rozie`re, “Proton conductivity of mesoporous MCM type of zirconium and titanium phosphates”, *Solid State Ionics*, vol. 125, pp.407–410,1999.



10.22214/IJRASET



45.98



IMPACT FACTOR:
7.129



IMPACT FACTOR:
7.429



INTERNATIONAL JOURNAL FOR RESEARCH

IN APPLIED SCIENCE & ENGINEERING TECHNOLOGY

Call : 08813907089  (24*7 Support on Whatsapp)